ARL-TR-7669 ● MAY 2016

US Army Research Laboratory

Corrosion-Mitigating, Bondable, Fluorinated Barrier Coating for Anodized Magnesium

by Joseph P Labukas, Noelle F Landers, Lindsey M Blohm, Victor Rodriguez-Santiago, and Thomas Parker

NOTICES

Disclaimers

The findings in this report are not to be construed as an official Department of the Army position unless so designated by other authorized documents.

Citation of manufacturer's or trade names does not constitute an official endorsement or approval of the use thereof.

Destroy this report when it is no longer needed. Do not return it to the originator.

ARL-TR-7669 ● MAY 2016

US Army Research Laboratory

Corrosion-Mitigating, Bondable, Fluorinated Barrier Coating for Anodized Magnesium

by Joseph P Labukas and Thomas Parker
Weapons and Materials Research Directorate, ARL

Noelle F Landers and Lindsey M Blohm
Oak Ridge Institute of Science and Education, Oak Ridge, TN

Victor Rodriguez-Santiago
US Naval Air Systems Command, Washington, DC

REPORT DOCUMENTATION PAGE

Form Approved
OMB No. 0704-0188

1. REPORT DATE *(DD-MM-YYYY)*	2. REPORT TYPE	3. DATES COVERED (From - To)
May 2016	Final	January–December 2015

4. TITLE AND SUBTITLE
Corrosion-Mitigating, Bondable, Fluorinated Barrier Coating for Anodized Magnesium

5a. CONTRACT NUMBER

5b. GRANT NUMBER

5c. PROGRAM ELEMENT NUMBER

6. AUTHOR(S)
Joseph P Labukas, Noelle F Landers, Lindsey M Blohm,
Victor Rodriguez-Santiago, Thomas Parker

5d. PROJECT NUMBER

5e. TASK NUMBER

5f. WORK UNIT NUMBER

7. PERFORMING ORGANIZATION NAME(S) AND ADDRESS(ES)
US Army Research Laboratory
ATTN: RDRL-WMM-C
Aberdeen Proving Ground, MD 21005-5066

8. PERFORMING ORGANIZATION REPORT NUMBER
ARL-TR-7669

9. SPONSORING/MONITORING AGENCY NAME(S) AND ADDRESS(ES)

10. SPONSOR/MONITOR'S ACRONYM(S)

11. SPONSOR/MONITOR'S REPORT NUMBER(S)

12. DISTRIBUTION/AVAILABILITY STATEMENT
Approved for public release; distribution is unlimited.

13. SUPPLEMENTARY NOTES

14. ABSTRACT
Enhanced barrier protection of magnesium (Mg) alloy AZ31B was achieved by coating oxidized Mg AZ31B H24 substrates with a perfluorinated silane. Then an atmospheric plasma treatment was used to promote adhesion of an epoxy topcoat to the silanized surface. This multistep process provides enhanced corrosion protection versus the untreated oxide as a result of accelerated corrosion testing via ASTM B117 (not shown) and electrochemical impedance spectroscopy. The adhesion of a top coat to this perfluorinated surface has been achieved and was tested using pull-off adhesion as described in ASTM D4541. Experimental work is ongoing for other anodized surfaces, various self-assembled monolayers, and alternative atmospheric plasma conditions.

15. SUBJECT TERMS
anodize, magnesium, corrosion, atmospheric plasma, surface modification

16. SECURITY CLASSIFICATION OF:			17. LIMITATION OF ABSTRACT	18. NUMBER OF PAGES	19a. NAME OF RESPONSIBLE PERSON
a. REPORT	b. ABSTRACT	c. THIS PAGE			Joseph P Labukas
Unclassified	Unclassified	Unclassified	UU	24	19b. TELEPHONE NUMBER (Include area code) 410-306-2989

Contents

List of Figures

List of Tables

Acknowledgments

The authors would like to acknowledge Kyo Cho for obtaining samples from TAG Corporation and to TAG for coating the substrates used in this work. We gratefully acknowledge Oak Ridge Institute of Science and Education (Oak Ridge, TN) for supporting Noelle Landers and Lindsey Blohm in this research.

INTENTIONALLY LEFT BLANK.

1. Introduction

Magnesium (Mg) alloys are of interest to the US Department of Defense and the automotive and aerospace industries because of their high strength-to-weight ratio. The use of Mg alloys as engineering materials for armor and structural components can provide a significant reduction in weight, thereby reducing fuel costs. From an environmental standpoint, the benefits of Mg alloys go beyond reduced fuel consumption from weight reduction in that most Mg alloys can be recycled. Although promising, these benefits are often offset by the poor corrosion resistance of most Mg alloys.

Mg corrosion proceeds by the following electrochemical reactions:

$$Mg \rightarrow Mg^{2+} + 2\ e^{-}\ . \quad (1)$$

$$2H_2O + 2e^{-} \rightarrow H_2 + 2OH^{-}\ . \quad (2)$$

Recent literature reports have verified this mechanism of Mg dissolution (Eq. 1) wherein 2 electrons are generated per atom of Mg to yield a divalent Mg cation.[1–8] The electrons produced during Mg dissolution are consumed at cathodic sites within an alloy to generate hydrogen gas from the reduction of water molecules (Eq. 2) present in the surrounding environment. Suppressing either of these reactions will lead to a decrease in the corrosion rate of an alloy. Similarly, the corrosion rate can also be controlled by alloying other elements with Mg. A recent review of alloying elements describes the effect of these elements on the corrosion behavior of Mg alloys.[9]

Along with the corrosion rate, the relative nobility of Mg alloys also changes through alloying additions. This is important from the standpoint of galvanic corrosion. Achieving an inherently corrosion-resistant Mg alloy does not guarantee that the corrosion rate of the alloy remains low when coupled to more-noble materials. Galvanic corrosion of Mg alloys and subsequent deterioration of the mechanical properties of an alloy are challenges often mitigated with engineering solutions that keep dissimilar materials insulated from one another in corrosive environments. Nonconducting organic materials (e.g., oils, waxes, and polymers) and metal oxides are most widely used as insulating barriers between dissimilar metals. For Mg, a typical insulating barrier to corrosion such as a mixed inorganic/oxide layer can be formed through plasma electrolytic oxidation (PEO). Magnesium alloy surfaces prepared by PEO are known to be porous, can develop cracks within the coating and along the coating metal interface, and the hard coating can be compromised by damage during impact. Protection of the anodized layer is often achieved by applying a subsequent polymeric coating such as an epoxy.

Although covering the anodized surface with a polymeric barrier helps seal the pores of the anodized layer, this barrier also produces a low-energy surface that is not amenable to bonding to a topcoat unless additional surface functionalization is performed. Nonthermal atmospheric pressure plasmas can modify a polymer surface through etching, introduction of chemical functional groups, and cross-linking to promote adhesion.[10] Depending on the reactive gas used and the exposure time, the surface modification of a low-energy surface can be tailored and primed for bonding by creating various functional groups (e.g., –OH and –COOH).

The focus of this work is 2-fold: 1) improve the barrier properties of electrolytically oxidized surfaces by chemically adsorbed perfluorinated silane monolayers and 2) modify this barrier-chemisorbed hydrophobic layer to enhance bonding of subsequent layers (e.g., a topcoat). We hypothesize that perfluorinated silanes chemisorbed onto an electrolytically oxidized Mg (AZ31B) surface can be chemically altered with an atmospheric plasma such that the layer will provide good adhesion of topcoats and increased barrier properties of the electrochemically derived oxide layer. Figure 1 shows the process used in modifying the anodized AZ31B surfaces. Chemical adsorption of silane molecules to oxidized AZ31B surfaces and the subsequent effects of atmospheric plasma modification on these surfaces were verified using water-contact-angle measurements. Barrier properties of coated substrates were investigated using electrochemical impedance spectroscopy (EIS). Adhesion of an epoxy topcoat to the plasma-modified silane layer was assessed by pull-off adhesion testing.

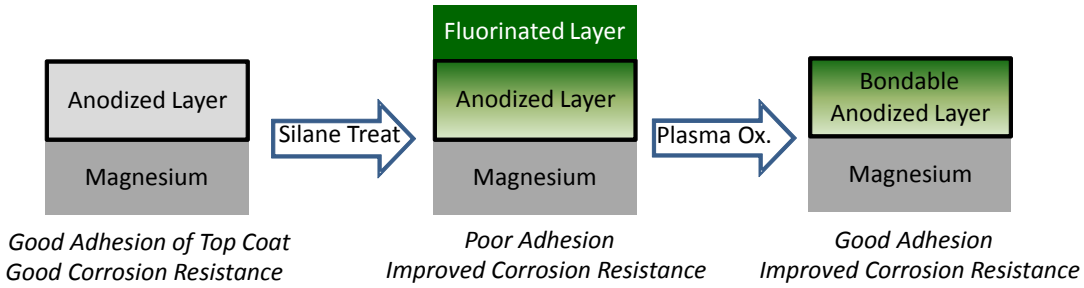

Fig. 1 Process for improving the corrosion resistance of anodized surfaces while maintaining adhesion possibility to a topcoat

2. Experimental Procedures

As received and used from the manufacturers were the following: 1H, 1H, 2H, 2H-perfluorodecyltriethoxysilane (Aldrich, 97%), ethanol (Decon, 200 proof), isopropyl alcohol (Sigma-Aldrich, ≥99.5%), and sodium chloride (NaCl) (VWR, 99%–100.5%). Water was purified to 18 MΩ cm using a Millipore system. Magnesium alloy AZ31B was obtained from Magnesium Elektron North America.

The alloy substrates were anodized by Technology Applications Group with 0.34–0.38 mil of the proprietary coating and tested as received.

2.1 Silane Deposition

Anodized AZ31B samples (4 × 6 × 1/4 or 1.5 × 1.5 × 1/4 inches) were soaked in a 1,000-mL solution of 1.1-mM 1H, 1H, 2H, 2H-perfluorodecyltriethoxysilane in ethanol for 42 min. The solution was decanted and replaced with another 1,000 mL of fresh silane solution for an additional 20 min. The solution volume for the small samples was 100 mL of 1.1-mM solution. After immersion, samples were removed, rinsed with ethanol and then deionized water, and then dried with a stream of nitrogen. To ensure that residual solvent had evaporated and that silane crosslinking had occurred, samples were allowed to sit uncovered in a fume hood for 1 h prior to electrochemical measurement, contact-angle measurement, or plasma treatment. Samples were stored in a fume hood for approximately 24 h before applying an epoxy topcoat.

2.2 Contact Angle Measurement

Contact angles were measured using a Rame-Hart Model 290 contact-angle goniometer. A droplet (~20 µl) was placed onto a surface and liquid was added to (or removed from) the droplet through a Gilmont screw-type syringe until the 3-phase contact line began advancing (or receding) across the surface. After advancement, contact angles were measured on each side of the drop. A minimum of 6 measurements was made across the sample surface. Contact angles less than 10° were difficult to measure accurately and are described throughout the text as having wet the surface.

2.3 Plasma Surface Modification

Plasma surface modification was performed using a custom-built atmospheric pressure plasma jet (APPJ). The plasma jet was a high-voltage (HV) electrode made from a 12-cm-long copper wire (1-mm outside diameter [OD]) embedded within an alumina dielectric (3-mm OD). The HV electrode was encapsulated within a 15-cm-long 0.30-mm-thick glass cylindrical tube (5-mm OD) with the ground electrode attached at the end of the tube, as shown in Fig. 2. A copper coil wrapped around the encapsulating glass cylindrical tube, positioned at the end of the HV electrode, acted as electrical ground. The HV electrode was positioned at the top of the glass tube, creating a 2.5-cm gap from the end of the HV electrode and nozzle/outlet of the cylindrical glass tube. The active discharge zone in the APPJ was confined to the length of the HV electrode while the afterglow region was

found to extend 2 cm. The plasma jet was powered by a microsecond-pulsed power supply that generated bipolar 30-kV pulses with a width of 30–40 μs. The peak power density of the plasma jet was measured to be 6.0–6.5 W cm^{-2}. An 8% duty cycle was used throughout the experiment. The power was kept constant throughout all experiments. A fixed helium flow rate to transport the precursor vapor throughout the study was set at 9,500 sccm. The setup also incorporated a 38- × 54- × 0.6-cm stainless steel moveable stage covered in glass used to mount the substrate. It provides a dynamic mode in addition to a static mode of treating large area substrates. The speed of the movable stage was adjusted as to provide a 5-s treatment time for a given area of the substrate.

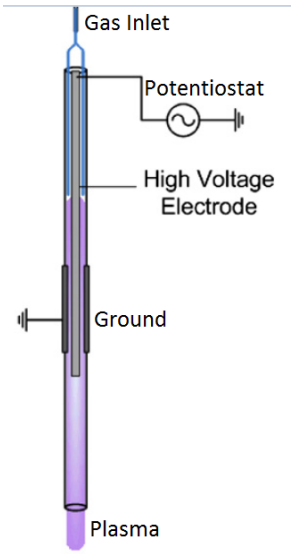

Fig. 2 Atmospheric pressure plasma jet used for surface modification

2.4 Electrochemical Impedance Spectroscopy (EIS)

EIS measurements were used to assess the barrier properties of anodized, perfluorinated, and plasma-modified surfaces with respect to each other. The electrochemical cell used was a Princeton Applied Research flat cell with a 1-cm^2 exposure area. The anodized AZ31B substrate was the working electrode, a platinum-coated niobium mesh was used as the counter electrode, and a saturated calomel electrode (SCE) was used as the reference. Uncoated AZ31B polished to a 600-grit finish using silicon carbide paper was used as a control sample and to determine the open circuit potential of the substrate. A Gamry reference 600 potentiostat was used to apply a 10-mV alternating-current amplitude over a frequency range of 0.01–10,000 Hz about the open circuit of the AZ31B substrate (~1.55 V vs. SCE) in quiescent 3.5% w/w NaCl (aqueous).

2.5 Adhesion Testing

Samples were coated with a MIL-DTL-53022D[11] Type IV epoxy primer to a dry film thickness of approximately 1.5 mil. The surface was allowed to cure for at least 154 days prior to performing pull-off testing to ensure full cure of the epoxy. Pull-off adhesion was performed in accordance with ASTM D4541[12] using a calibrated PosiTest Adhesion Tester (DeFelsko, PosiTest AT-A). The epoxy surface and the base of the aluminum dollie was wiped clean with isopropyl alcohol using a Kimwipe prior to pull-off testing. Aluminum dollies with a 20-mm diameter were glued to the epoxy surface using a cyanoacrylate adhesive (Gorilla Impact Tough formula). Samples were allowed to cure for at least 24 h before the pull-off test was performed. Only one aluminum dollie was glued to each sample at a time to ensure the shock associated with pulling a dollie from the sample would not affect the adhesion of other dollies. One pull-off was performed each day per sample.

2.6 Scanning Electron Microscopy (SEM)

The surface of the anodized Mg alloy AZ31B, as received from Technology Applications Group, was characterized by SEM (Hitachi 4700). The microscope was operated at 2.0 kV.

2.7 Rutherford Backscattering Spectroscopy (RBS)

An NEC Pelletron (Model 5SDH-2) was used to conduction RBS analysis of the as received and treated, anodized Mg alloy AZ31B (Technology Applications Group). Singly charged alpha particles with an energy of 2 MeV were used with a sample beam current of approximately 20 nA. A cryopumped analysis chamber was equipped with a surface barrier detector with a specified energy resolution of 12 keV and a measured energy resolution of 14 keV that includes electronic noise. The RBS spectra was analysis using SIMNRA software version 6.06.

3. Results and Discussion

Trialkoxysilanes are known to undergo condensation reactions on hydroxyl-terminated surfaces to form self-assembled monolayers (SAMs) (Fig. 3).[13]

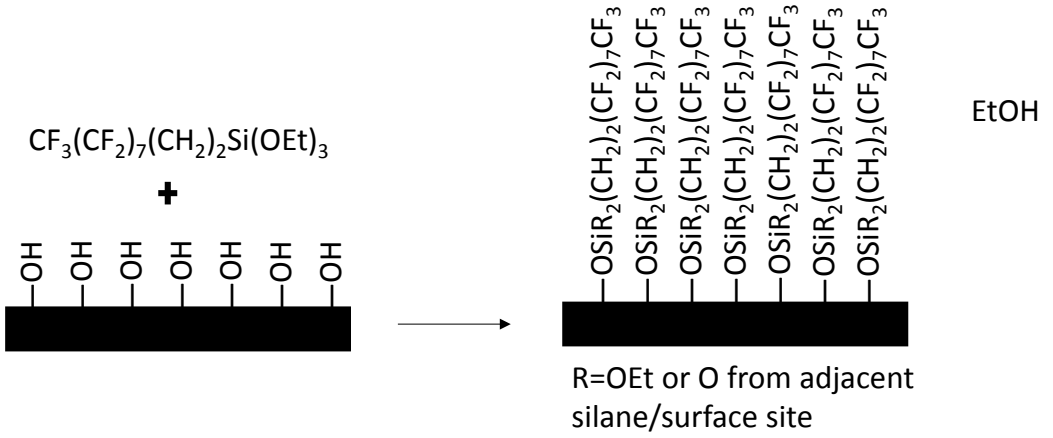

Fig. 3 Self-assembly of perfluorinated silane on a hydroxyl terminated surface

The self-assembly process results in covalent attachment of the silane head group to the surface. After the chemical reaction is complete, the oleophobic "tails" of the silane molecule are oriented upward and form the modified samples surface. The exposed chemical functionality of these tails, the packing density of the SAM, and the chain length of the silane molecule all play a role in establishing the free energy of the new surface. The surface free energy is commonly gauged by measuring the contact angle of a liquid on the substrate as depicted in Fig. 4.

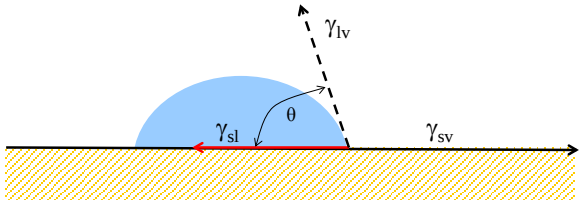

Fig. 4 Liquid drop on a substrate

The relationship between these surface free energies and wettability is most commonly described by Young's equation.

$$\gamma_{lv} \cos \theta = \gamma_{sv} - \gamma_{sl}, \quad (3)$$

where γ_{lv} is the liquid vapor interfacial free energy, γ_{sv} is the solid vapor interfacial free energy, and γ_{sl} is the solid/liquid interfacial free energy.[14]

Contact-angle measurements of anodized AZ31B surfaces, perfluorinated surfaces, and plasma-modified perfluorinated surfaces are shown in Table 1. Using water as a probe liquid, the as-received anodized surfaces have a low water contact angle (22.0°), which is expected for a surface functionality likely consisting of a mixture of oxide and hydroxide groups that can interact via hydrogen bonding with water. After silane treatment with the perfluorinated silane, the contact angle of the

substrate increases to a nearly superhydrophobic value (148.3°) consistent with the newly formed fluorine containing hydrophobic SAM formed on a rough surface. The atmospheric plasma treated, silanized surface (i.e., generated to incorporate hydrophilic groups that promote adhesion of a subsequent topcoat) had wettable surfaces with lower water contact angles (54.4°). These wettability measurements reveal that the surface has been modified from hydrophilic to superhydrophobic and back to hydrophilic.

Table 1 Contact angles of water on treated AZ31B surfaces

Contact Angle	Anodized AZ31B (°)	Anodized + silanized (°)	Anodized + silanized + plasma treatment (°)
Advancing (θ_a)	22.0 (+/–6.5)	148.3 (+/–13.8)	54.4 (+/– 8.8)
Receding (θ_r)	Wet	Wet	Wet

Water-contact-angle measurement probes approximately 5 Å into a SAM on a flat surface[15]; however, it does not probe chemical functionality throughout the bulk anodized layer. One hypothesis being tested in this research is that silane molecules permeate the porous anodized layer and remain within the anodized layer after the outermost surface has been modified with an atmospheric plasma. A SEM of the porous electrolytically oxidized AZ31B sample (as received) is shown in Fig. 5.

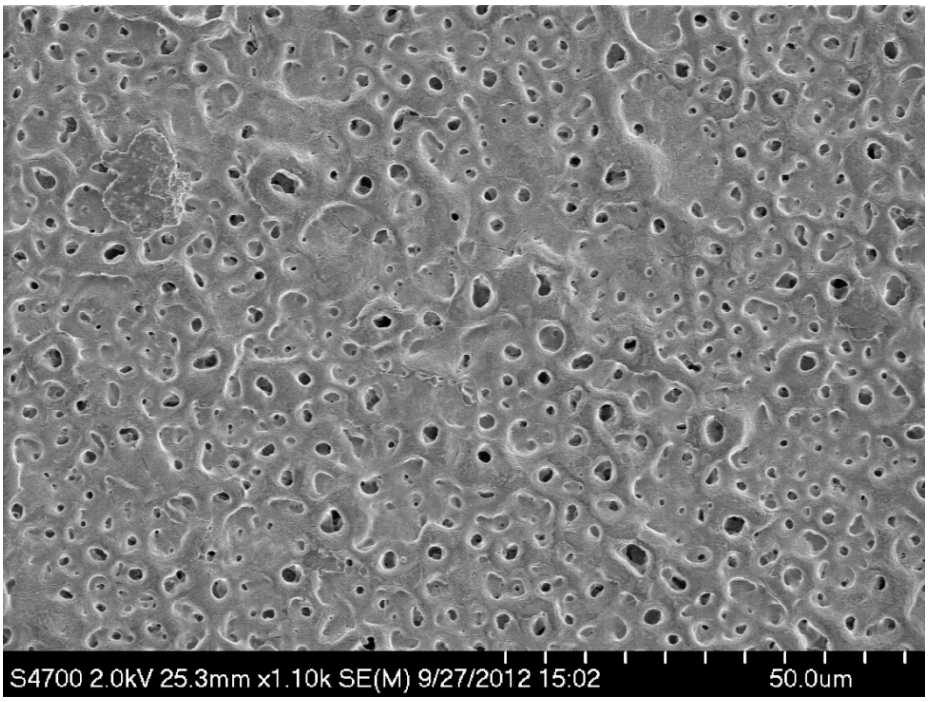

Fig. 5 SEM of anodized AZ31B as received

To test this hypothesis, the barrier properties of the untreated and perfluorinated surfaces (before and after plasma modification) were probed using EIS. Figure 6 shows the impedance spectra for AZ31B in anodized, anodized/silanized, and anodized/silanized/plasma treatment conditions. Both the anodized/silanized and anodized/silanized/plasma treated samples showed impedance values orders of magnitude higher than the anodized sample. These preliminary results indicate that the barrier properties afforded by the silane coating are not compromised by the plasma treatment. It can be inferred that the silane layer covers the pores of the anodized layer, and the plasma treatment is only modifying the outer layers of the coating. This would allow enough surface modification to allow reactions with the topcoat but still retain enhanced barrier properties.

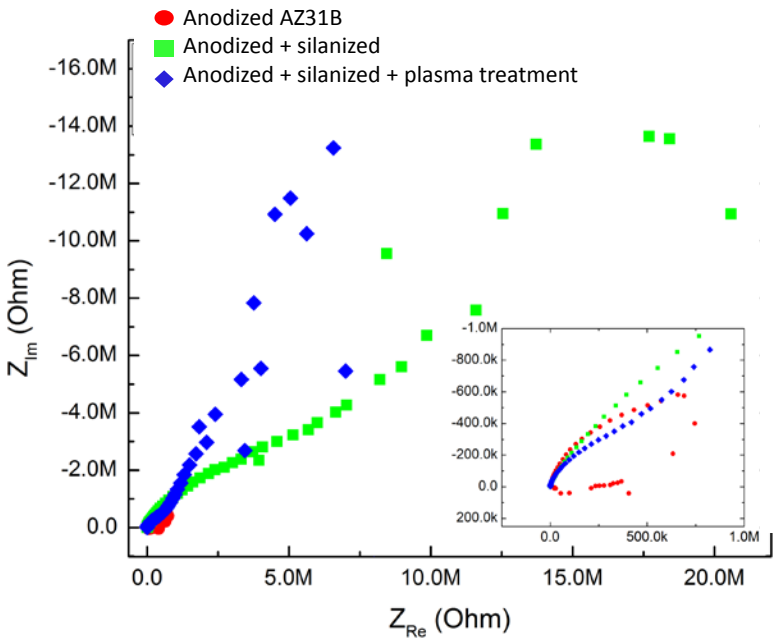

Fig. 6 EIS of various surface treatments to AZ31B

Application of an adherent coating to the anodized layer is important for long-term durability and final appearance of an asset. Adhesion to all 3 systems was tested by applying a MIL-DTL-53022[8] Type IV standard epoxy topcoat to each of the substrates and performing pull-off adhesion tests. The results of these measurements are shown in Table 2. Images of the coated substrate after testing appear in Fig. 7.

Table 2 Pull-off adhesion strength on various anodized Mg AZ31B surfaces

Test No.	Anodized AZ31B (psi)	Anodized + silanized (psi)	Anodized + silanized + plasma treatment (psi)
1	343	524	659
2	1,026	374	818
3	569	441	534
4	1,617	461	745
5	1,198	573	865
6	796	368	469
7	822	688	764
Average	910 (+/–419)	490 (+/–115)	693 (+/–147)

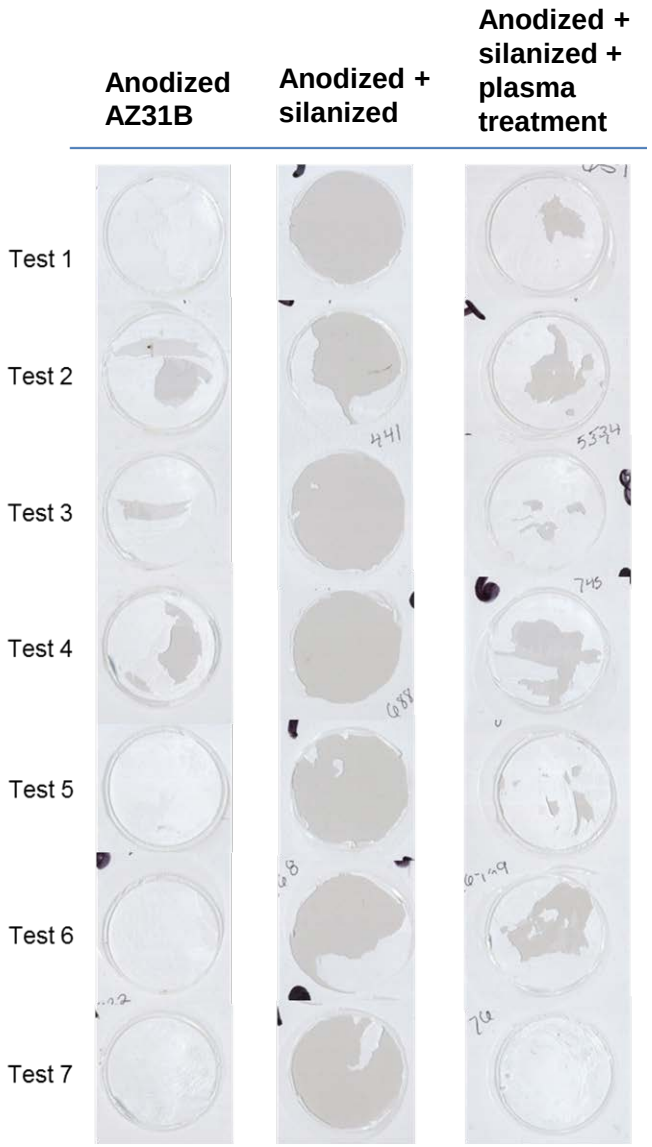

Fig. 7 Photographs of the coated substrate after adhesion testing

Using the available data, it is difficult to correlate pull-off strength to the failure mode. Further surface chemical analysis is required to determine the chemical functionality of material residues across the pulled-apart surfaces. However, assuming adhesive failure was the predominant mode of failure, the percentage of adhesive failure based on exposed surface area was measured using National Institutes of Health software Image J. The dark areas closely resemble unmodified anodized samples in the as-received state. The percentage of darkened areas (assumed to be locations where adhesive failure occurred) is shown in Table 3. As expected, the perfluorinated silane treatment alone yielded the lowest pull-off adhesion and appeared to fail almost exclusively at the epoxy/modified substrate interface (Fig. 7). Intermediate values for pull-off adhesion on the control sample and plasma modified samples indicate that adhesion is good and there is a mixed mode of failure for both surfaces.

Table 3 Adhesive failure of epoxy-coated treated Mg substrates

Test No.	Approximate surface area of adhesive failure		
	Anodized AZ31B (%)	**Anodized + silanized (%)**	**Anodized + silanized + plasma treatment (%)**
1	0[a]	100	12
2	27	61	24
3	10	100	6
4	23	100	36
5	0[a]	99	5
6	0[a]	71	36
7	0[a]	93	0

[a]Failure appears to be predominantly cohesive within the epoxy.

The RBS spectra of the silanized and as-received electrolytically oxidized Mg samples are shown in Fig. 8. The x-axis of the data is in units of channels where the conversion to the detected particle energy is given by E(keV) = (1.36 keV/Channel) * Channel # + 60 keV. The y-axis gives the normalized counts, which were normalized to the area around channel 400. The analysis of the silanized sample indicate that there is a 15-nm surface layer that has an enhanced fluorine content on the order of 15 at% (Fig. 8 , left graph inset). The as-received sample shows a uniform fluoride content of 8.4 atomic percent with no surface peak present. The surface fluorine peak in the silanized sample indicates the presence of the silane at the surface of the sample (~15 nm) without further penetration into the bulk of the anodized layer.

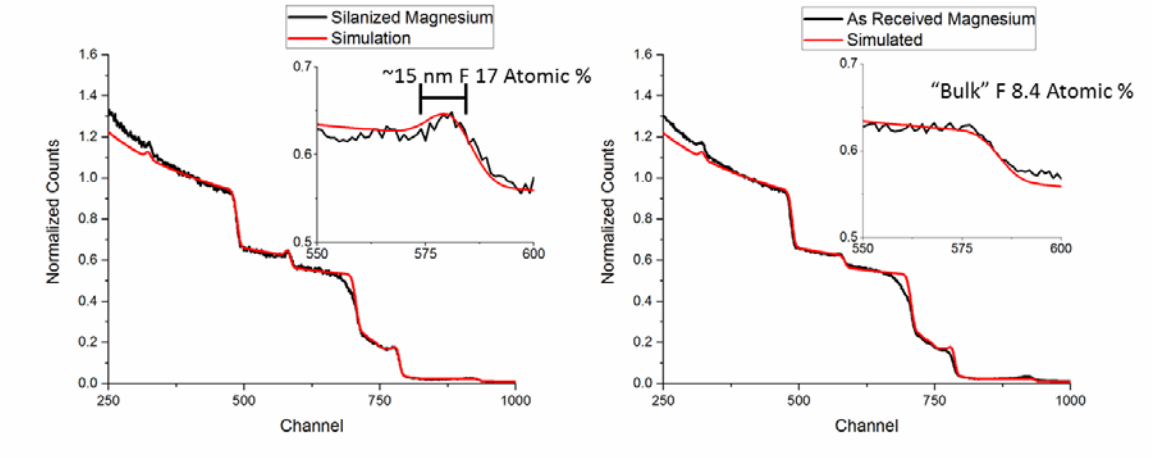

Fig. 8 RBS data of the anodized Mg samples coated with (left) perfluorinated silane and (right) as-received with a plasma electrolytically formed oxide layer

4. Conclusions

Electrolytically oxidized surfaces can be modified with a perfluorinated silane to yield superhydrophobic surfaces with enhanced barrier properties. Enhanced barrier properties typically translate to enhanced corrosion resistance. In our system the enhanced corrosion resistance is implied from EIS measurements. Chemisorption of perfluorinated silane into the PEO AZ31B surfaces results in low-energy surfaces with and poor adhesion of an epoxy topcoat. Atmospheric plasma treatment enhanced adhesion of an epoxy topcoat, as observed using pull-off adhesion testing, while maintaining the apparent barrier properties measures via EIS. This chemisorption and subsequent surface modification provides a new level of corrosion protection for PEO surfaces and perhaps lightweight alloys with a robust native oxide.

5. References

1. Thomas S, Medhekar NV, Frankel GS, Birbilis N. Corrosion mechanism and hydrogen evolution on Mg. Current Opinion in Solid State and Materials Science. 2015;19(2):85–94.

2. Bland LG, King AD, Birbilis N, Scully JR. Assessing the corrosion of commercially pure Mg and commercial AZ31b by electrochemical impedance, mass-loss, hydrogen collection, and inductively coupled plasma optical emission spectrometry solution analysis. Corrosion. 2015;71:2128–2145.

3. Kirkland, NT. Williams G, Birbilis N. Observations of the galvanostatic dissolution of pure M. Corrosion Science. 2012;65:50150.

4. Rossrucker L, Mayrhofer KJ, Frankel GS, Birbilis N. Investigating the real time dissolution of magnesium using online analysis by ICP-MS. Journal of the Electrochemical Society. 2014;161(3):C115–C119.

5. Rossrucker L, Samaniegob A, Grote JP, Mingers AM, Laska CA, Birbilis N, Frankel GS, Mayrhofer KJ. The pH dependence of magnesium dissolution and hydrogen evolution during anodic polarization. Journal of the Electrochemical Society. 2015;162(7):C333–C339.

6. Williams G, Birbilis N, McMurray HN. The source of hydrogen evolved from a Mg anode. Electrochemistry Communications. 2013;36:1–5.

7. Frankel GS. Samaniego A, Birbilis N. Evolution of hydrogen at dissolving magnesium surfaces. Corrosion Science. 2013(70):104–111.

8. King AD, Birbilis N, Scully JR. Accurate electrochemical measurement of magnesium corrosion rates: a combined impedance, mass-loss and hydrogen study. Electrochimica Acta. 2014;121:394–406.

9. Gusieva KC, Davies HJ, Scully R, Birbilis N. Corrosion of magnesium alloys: the role of alloying. International Materials Reviews. 2015;60(3):169–194.

10. Rodriguez-Santiago V, Bujanda AA, Stein BE, and Pappas DD. Atmospheric plasma processing of polymers in helium-water vapor dielectric barrier discharges. Plasma Process and Polymers. 2011;8:631,

11. MIL-DTL-53022D. Primer, epoxy coating, corrosion inhibiting lead and chromate free. Aberdeen Proving Ground (MD): Army Research Laboratory (US); 2010 May 7.

12. ASTM D4541-09. Standard test method for pull-off strength of coatings using portable adhesion testers. West Conshohocken (PA): ASTM International; 2002.

13. Plueddemann E. Silane coupling agents. New York (NY): Springer; 1991.

14. Young, T. An essay on the cohesion of fluids. Phi Trans R Soc Lond. 1805;95:65–87.

15. Ferguson GS, Whitesides GM. Thermal reconstruction of the functionalized interface of polyethylene carboxylic acid and its derivatives. In: Schrader ME, Loeb GI, editors. Modern approaches to wettability – theory and applications. New York (NY): Plenum; 1992. pp 143–177.

List of Symbols, Abbreviations, and Acronyms

APPJ	atmospheric pressure plasma jet
EIS	electrochemical impedance spectroscopy
HV	high voltage
Mg	magnesium
NaCl	sodium chloride
OD	outer diameter
PEO	plasma electrolytic oxidation
SAM	self-assembled monolayer
SCE	saturated calomel electrode
SEM	scanning electron microscopy

1 (PDF) DEFENSE TECHNICAL INFORMATION CTR DTIC OCA

2 (PDF) DIRECTOR US ARMY RESEARCH LAB RDRL CIO LL IMAL HRA MAIL & RECORDS MGMT

1 (PDF) GOVT PRINTG OFC A MALHOTRA

1 (PDF) DIR USARL RDRL WMM C J LABUKAS

INTENTIONALLY LEFT BLANK.